PROCEEDINGS, 43rd Workshop on Geothermal Reservoir Engineering
Stanford University, Stanford, California, February 12-14, 2018
SGP-TR-213

Experimental Design for Hydrofracturing and Fluid Flow at the DOE Collab Testbed

Joseph P. Morris[1], Patrick Dobson[2], Hunter Knox[3], Jonathan Ajo-Franklin[2], Mark D. White[4], Pengcheng Fu[1], Jeffrey Burghardt[4], Timothy J. Kneafsey[2], Douglas Blankenship[3], and EGS Collab Team[5]

Atmospheric, Earth, and Energy Division, Lawrence Livermore National Laboratory, Livermore, CA 94551

Lawrence Berkeley National Laboratory, Berkeley, CA 94720

Sandia National Laboratory, Albuquerque, NM 87123

Pacific Northwest National Laboratory, Richland, WA 99352

Email: morris50@llnl.gov

Keywords: Hydraulic fracturing, enhanced geothermal system, EGS, SURF

ABSTRACT

We describe our overall objectives and approach to designing the first experimental testbed of the EGS Collab project. This first phase of the project entails site characterization, drilling, stimulating, and performing flow tests using largely horizontal wellbores in phyllite of the Precambrian Poorman Formation, at the Sanford Underground Research Facility (SURF), located at the former Homestake Gold Mine, in Lead, South Dakota. This suite of hydrofracture and flow test experiments builds upon the stress and hydrofracture experiments performed at the nearby kISMET (permeability (k) and Induced Seismicity Management for Energy Technologies) site. While this paper provides an overview of the experiment design and design process, separate papers will describe the characterization of the site, the monitoring system, and other aspects of the project.

1. INTRODUCTION[1]

Enhanced or engineered geothermal systems (EGS) offer tremendous potential as an indigenous renewable energy resource supporting the energy security and sustainability of the Nation. The Department of Energy (DOE) Geothermal Technologies Office has a robust R&D program directed at EGS (e.g., Ziagos et al., 2013) that includes several EGS field demonstration sites, as well as the Frontier Observatory for Research in Geothermal Energy (FORGE), the DOE's flagship EGS research effort. FORGE, which is currently in the Phase II site - selection process (e.g., Blankenship et al., 2017; Allis et al., 2016), will produce a full - scale field laboratory with a focus on developing, testing, and validating technologies to improve EGS reservoir access, creation, productivity, and sustainability. While FORGE will develop the most heavily-instrumented EGS research site to - date, the target geothermal system will be deep and hot (depth exceeding 1.5 km) and thus the associated cost of borehole access will necessarily limit process observations. The high cost and limitations of access inherent to deep reservoirs place severe limits on our ability to observe fundamental processes critical to EGS development such as fracture propagation and sustainable fluid flow for heat extraction. The success of FORGE will be accelerated by near - term research and development activities, testing in readily-accessible underground facilities at intermediate (on the order of 10 m) scales that can refine our understanding of rock mass response to stimulation, and provide a test bed for the validation of thermal-hydrological mechanical - chemical (THMC) modeling approaches as well as novel monitoring tools.

The EGS Collab project is a multi - lab and -university collaborative research project focusing on intermediate - scale EGS reservoir generation processes and related model validation at crystalline rock sites. Cooperative research under the EGS Collab project will provide a foundation of knowledge and modeling capability that forms a bridge to meeting the challenges of FORGE. The EGS Collab project provides researchers the ability to address and meet the fundamental challenges of understanding and predicting permeability enhancement and evolution in crystalline rocks, including how to produce sustained and distributed permeability for heat extraction from the reservoir by generating new fractures as well as stimulating existing fractures. The scale of the EGS Collab project fracture

[5] J. Ajo-Franklin, S.J. Bauer, T. Baumgartner, K. Beckers, D. Blankenship, A. Bonneville, L. Boyd, S.T. Brown, J.A. Burghardt, T. Chen, Y. Chen, K. Condon, P.J. Cook, P.F. Dobson, T. Doe, C.A. Doughty, D. Elsworth, J. Feldman, A. Foris, L.P. Frash, Z. Frone, P. Fu, K. Gao, A. Ghassemi, H. Gudmundsdottir, Y. Guglielmi, G. Guthrie, B. Haimson, A. Hawkins, J. Heise, C.G. Herrick, M. Horn, R.N. Horne, J. Horner, M. Hu, H. Huang, L. Huang, K. Im, M. Ingraham, T.C. Johnson, B. Johnston, S. Karra, K. Kim, D.K. King, T. Kneafsey, H. Knox, J. Knox, D. Kumar, K. Kutun, M. Lee, K. Li, R. Lopez, M. Maceira, N. Makedonska, C. Marone, E. Mattson, M.W. McClure, J. McLennan, T. McLing, R.J. Mellors, E. Metcalfe, J. Miskimins, J.P. Morris, S. Nakagawa, G. Neupane, G. Newman, A. Nieto, C.M. Oldenburg, W. Pan, R. Pawar, P. Petrov, B. Pietzyk, R. Podgorney, Y. Polsky, S. Porse, S. Richard, M. Robertson, W. Roggenthen, J. Rutqvist, D. Rynders, H. Santos-Villalobos, P. Schwering, V. Sesetty, A. Singh, M.M. Smith, H. Sone, C.E. Strickland, J. Su, C. Ulrich, N. Uzunlar, A. Vachaparampil, C.A. Valladao, W. Vandermeer, G. Vandine, D. Vardiman, V.R. Vermeul, J.L. Wagoner, H.F. Wang, J. Weers, J. White, M.D. White, P. Winterfeld, T. Wood, H. Wu, Y.S. Wu, Y. Wu, Y. Zhang, Y.Q. Zhang, J. Zhou, Q. Zhou, M.D. Zoback

stimulation and fluid flow experiments will allow proximal monitoring through multiple boreholes, leading to high-resolution geological and geophysical characterization of the rock mass before, during, and after stimulation. Advanced modeling is being utilized to assist in the design of field tests aimed at providing the key perturbation-response feedback information needed to constrain mechanistic models of coupled THMC processes (e.g., the degree to which shear offset on an existing fracture increases permeability of the fracture). Data on fracture permeability enhancement mechanisms (e.g., slip on existing fractures, new fracture generation, and mixed mode fracturing) will be gathered through fracturing and fluid-flow experiments. These observations will provide the THMC modeling community with a rich data set that can in turn be used to validate the capabilities of predictive models that will be employed to support FORGE.

In this paper we will summarize the process followed for determining the locations and orientations of stimulation, flow, and monitoring boreholes. We will provide a summary of the planned geophysical monitoring and flow tests. The final design for this first testbed has balanced the validation goals of the experiment with achieving successful stimulation and intersection with a producing well. The rapid design phase leveraged close teamwork among stimulation, flow, and modeling teams along with rapid cross-verification and peer-review among all participants.

2. OVERVIEW OF SURF

Evaluation of site criteria led the team to choose the Sanford Underground Research Facility (SURF) in South Dakota as the first EGS Collab project experimental site. As a mined underground research laboratory, SURF offers advantages to allow the EGS Collab project work to move forward with relative ease, including cost-effective proximal monitoring of a crystalline rock mass before, during, and after stimulation through multiple boreholes drilled from an underground tunnel (i.e., a mine drift). A priority was placed on assuring the selected site had accessible rock under realistic in situ stress conditions and that these conditions could be assessed at minimal cost. While moderate temperature would be advantageous, and SURF is at low temperature (~30-35° C) at the designated testing depth, locating a site that offers both realistic temperatures and stress involves relatively deep drilling, which is costly and does not facilitate detailed monitoring and would thereby obviate the ability to achieve the EGS Collab objectives. Several options exist to replicate temperature-induced effects in the field (e.g., using chilled or heated brines to induce a differential temperature) or via complementary laboratory experiments involving high-temperature measurements; similar options do not exist to replicate stress. At depths of approximately 1500 m, SURF satisfies the stress criterion.

As a former working mine and current active site for physics research (Heise, 2015), SURF is well-characterized (e.g. Hart et al., 2014) with robust installed infrastructure (e.g., ventilation, power, water, and internet) and maintains an excellent staff dedicated to scientific research support, in addition to health and safety practices and all necessary environmental permitting. The experiences and relationships developed by many of the EGS Collab project team members in the recent (2015-2016) kISMET project (Oldenburg et al., 2016; 2017; Wang et al., 2017; Zhou et al., 2017, Figure 1) at SURF ensure minimal lag time in site-selection at SURF and carrying out the proposed field experiments (Fig. 1).

Figure 1: Underground work at SURF under the kISMET project.

3. DEVELOPMENT OF THE BASIC TESTBED DESIGN

The greatest technical challenge is the inherent uncertainty in the subsurface. Our goal is to design a robust stimulation and flow-through experiment to enable model validation. However, we cannot know everything about the rock mass and uncertainty in stress orientation and magnitude along with the unknown presence of preexisting discontinuities that can dominate system response. Consequently, our first objective was to select a specific location at SURF consistent with a borehole geometry that would best facilitate direct observation of stimulation via hydraulic fracturing and subsequent flow-through tests. However, such advantages must also be weighed against logistical necessities (access to transportation, power, water, internet, etc.) that vary with location throughout the mine.

The first experiment is intended to stimulate the rock via hydraulic fracturing and so the basic layout of the test bed is dictated to first order by the orientation and size of the hydraulic fractures. Stress orientation is well known to dictate hydraulic fracture orientation in the absence of strong heterogeneity or preexisting fractures (Hubbert and Willis, 1957). In fact, hydraulic fracturing is often used to infer stress orientation and the magnitude of the minimum horizontal stress. Field measurements of the stress field by hydraulic fracturing showed that the minimum horizontal stress at the kISMET site (Oldenburg et al., 2017; Wang et al., 2017) averages 21.7 MPa (3146 psi) pointing approximately N-S (356 degrees azimuth) and plunging slightly NNW at 12 degrees from horizontal. Figure 2 shows a hypothetical testbed geometry utilizing a corner between two drifts to provide access to both suitably oriented stimulation, production, and observation boreholes. This drift geometry facilitates deploying observation boreholes both parallel and perpendicular to the stimulated fractures. Such a location was sought during site selection at SURF; however, we were unable to identify such an arrangement within the portions of SURF currently serviced with utilities necessary for the experiment.

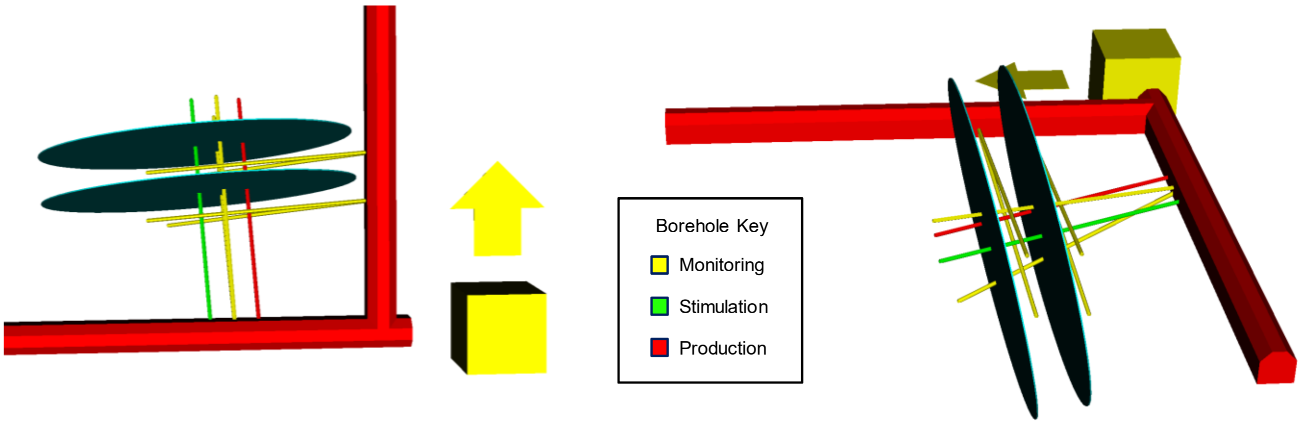

Figure 2: Potential test bed geometry at an intersection of two drifts. The arrow indicates North and the 10 m yellow cube is included as a scale indicator. The disks correspond to idealized hydraulic fractures, opening against the minimum horizontal stress with a design radius of 20 m.

It was subsequently realized that siting the first experiment in a drift at an angle to the stress field provides the advantage that a single drift can be used effectively to place the boreholes such that they straddle the stimulation zone by locating the borehole collars sufficiently distant along the length of the drift. In fact, the kISMET site is located in a drift of such orientation. In addition, this location has been demonstrated to have suitable supporting infrastructure. Consequently, the kISMET site was selected, and borehole layouts proposed (see Figure 3). One disadvantage of this geometry is that the stimulation borehole must be longer in order to achieve a given distance from the drift. However, the 60 m boreholes shown in Figure 3 were within the project budget and achieve sufficient standoff from the drift to serve our objectives. Furthermore, the production borehole lies between the stimulation borehole and the drift and should mitigate against excessive growth toward the drift (see later discussion).

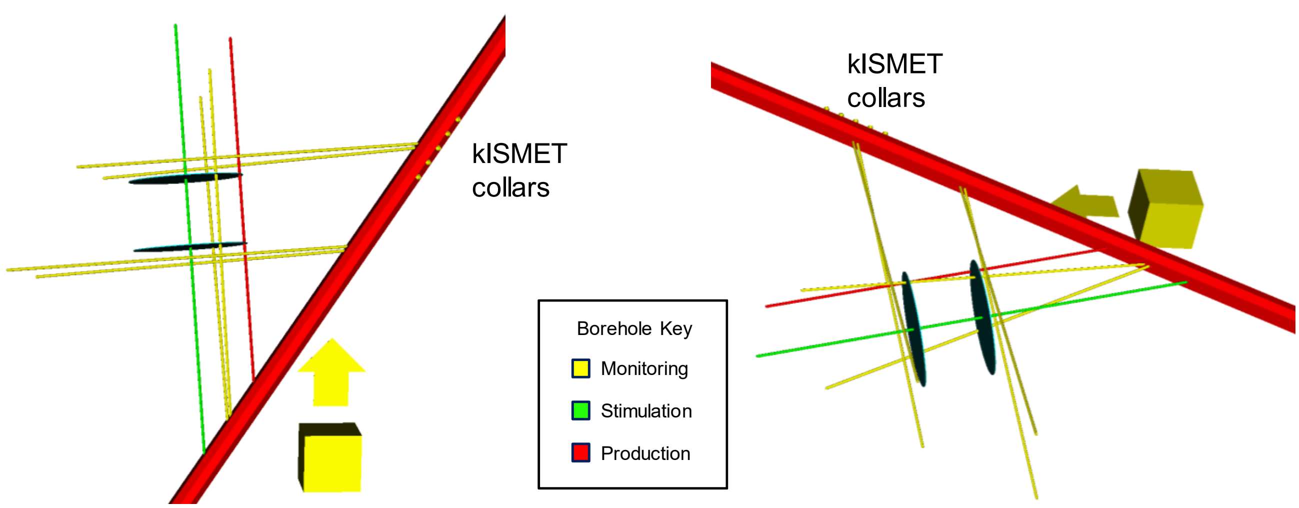

Figure 3: Potential test bed geometry utilizing a single drift running at an angle to the principal stress directions. The arrow indicates North and the 10 m yellow cube is included as a scale indicator. The disks correspond to idealized hydraulic fractures, opening against the minimum horizontal stress with a design radius of 20 m.

The basic design of Experiment I shown in Figure 3 includes a number of largely horizontal wells, including a stimulation/injection well, a production (flow-back) well, and several monitoring wells, from the West Access Drift of SURF at 4850 ft (1478 m) below ground in phyllite of Precambrian Poorman Formation. The orientations of the wells were based on in situ stress measurements made in the kISMET test. The stimulation well is along the interpreted minimum principal stress (S_{hmin}) direction from kISMET, N4°W with a 12° down dip. Because the drift axis orients N33.5°E, the angle between the stimulation well axis and the drift axis is approximately 37.5° on a plan view. Multiple hydraulic fractures will be initiated in the stimulation well, and they are expected to be perpendicular to the wellbore axis if the perturbation to the in situ stress from the drift proves to be minimal. In the circulation experiment, this well will be used as the injection well; the production well, through which the circulation fluid returns, is largely parallel to the stimulation/injection well, with a 10 m offset toward the drift direction. The following sections will discuss the stimulation, flow test, and associated geophysics.

4. STIMATULION EXPERIMENTAL DESIGN

In this section we discus modeling and other considerations that went into the initial design of the stimulation experiment. Companion papers will discuss these matters in greater detail.

4.1 Preliminary Hydraulic Fracture Modeling

In this section, we discuss an example of the preliminary modeling and some relevant, comparable field tests that have been used to guide the experimental design for the first experiment. Results like these (presented here and in White et al. (2017) and Huang et al. (2017)) help guide not only the monitoring network design (i.e. where sensors need to be located), but also help inform test criteria such as stimulation/flow rates and expected breakdown pressures. In this case, we use the Oldenburg et al. (2016) (a.k.a. kISMET report) formation properties for initial model parameters (see Table 1). Table 2 lists properties that we have selected to be representative of our planned stimulation (fluid viscosity and pumping rate) along with the typical rock toughness value used in the literature when data is absent.

Table 1: Formation properties obtained from Oldenburg et al. (2016)

Property	Value
Rock Young's modulus, E	71.4 GPa
Rock Poisson's ratio, v	0.22
Min. horizontal principal stress, S_{hmin}	20 MPa

Table 2: Representative values for material properties obtained from general literature.

Property	Value
Rock critical stress intensity factor, K_{IC}	1.0 MPa(m)$^{0.5}$
Fluid viscosity, μ	0.001 Pa s
Fluid density, ρ	1000 kg/m^3

The propagation of hydraulic fractures will be within the so-called toughness-dominated regime, viscosity-dominated regime, or somewhere between these two extreme cases depending on the main mode of energy dissipation (Detournay, 2004). According to Detournay (2004), the dimensionless toughness of a penny-shaped fracture is

$$\mathcal{K} = K'\left(\frac{t^2}{\mu'^5 Q_0^3 E'^{13}}\right)^{1/18}$$

and the dimensionless viscosity is

$$\mathcal{M} = \mu'\left(\frac{Q_0^3 E'^{13}}{K'^{18} t^2}\right)^{1/5}$$

where $K' = 4(2/\pi)^{0.5} K_{IC}$, $\mu' = 12\mu$ and $E' = E/(1-\nu^2)$.

Based on Sneddon (1946) and Sneddon and Elliot (1946) and the stress intensity factor for a penny-shaped fracture, we can derive the fracture length R, maximum aperture w, and net pressure ΔP of a penny-shaped hydraulic fracture in the toughness-dominated regime as:

$$R(t) = \left(\frac{3Q_0 t E'}{8K_{IC}\sqrt{\pi}}\right)^{2/5}$$

$$w(t) = \left(\frac{12Q_0 t K_{IC}^4}{\pi^3 E'^4}\right)^{1/5}$$

$$\Delta P = \frac{\pi w E'}{8R}$$

The closed-form solutions for the viscosity-dominated regime provided by Nolte (2000) are:

$$R(t) = 0.52\left(\frac{Q_0^3 E'}{\mu}\right)^{1/9} t^{4/9}$$

$$w(t) = 2.17\left(\frac{Q_0^3 \mu^2}{E'^2}\right)^{1/9} t^{1/9}$$

If we consider an injection rate of 0.1 L/s, combined with the parameters in Tables 1 and 2, we find that $\mathcal{K} = 1.44$ and $\mathcal{M} = 0.27$, indicating that the propagation is largely in the toughness-dominated regime while viscous dissipation plays a secondary role. After 10 mins of injection (with 60 L injected), the toughness-dominated solution predicts a radius of 15.5 m and an aperture of 118 microns, whereas the viscosity-dominated solution predicts a radius of 14.4 m and an aperture of 169 microns. The toughness-dominated solution assumes pressure in static equilibrium and the equilibrium net pressure is 225 kPa. Note that after 100 L of fluid are injected, the predicted radii are 19.8 m and 17.1 m for the toughness- and viscosity-dominated solutions, respectively. For comparison, the previous kISMET stimulation involved a net injection of 28.1 liters (Oldenburg et al., 2016, page 90) and might be expected to have a radial extent of 11.4 m for the toughness-dominated solution. Unfortunately, there was no independent verification of the dimensions of the induced fractures from the kISMET experiment (Oldenburg et al., 2016).

To provide some confidence for the experiment design, it is useful to compare our preliminary predictions with previous field observations in comparable formations for which acoustic emission (AE) data are available. In June 2015, a series of hydraulic fracturing tests were conducted at Äspö (Zang et al., 2017). The goal of the tests was to determine how aspects of the injection protocol can influence the generation of AE. The experiments employed pumping rates between 0.01 and 0.08 L/s with a typical total volume injected of 10 liters (see Zang et al. 2017, Table 3). The AE observations performed during these tests indicate the fractures have a radius of approximately 6 m (see Zang 2017, Figure 8). Although Zang et al. (2017) do not report any moduli for the formation, other sources indicate values similar to those reported for the kISMET project (see Juvonen, 2002, Table 4). Using the same baseline properties in Tables 1 and 2 and 0.1 L/s injection rate, 10 L of injected fluid is predicted to result in a 7.6 m and 7.9 m radius fracture for the toughness- and viscosity-dominated solutions, respectively. These results are in good agreement with the observed microseismic observation of 6 m mentioned previously, giving us confidence in our scoping calculations for the SIGMA-V experiment. Note that these results assume no leak-off, which would decrease fracture length.

4.2 Influence of Perturbed Stress Around Stimulation Borehole

One concern for developing a fracture that will be straightforward to model is to avoid near wellbore complexity due to perturbed stresses near the borehole. To avoid this effect, the team is scribing the borehole to produce a fracture initiation notch (e.g., Jeffrey et al., 2015) prior to fracturing to help ensure the proper near wellbore orientation. Initial modeling of this process is being done to reduce the fracture initiation pressure (also known as the formation breakdown pressure) so that is below the intermediate stress value (which is estimated to be around 35 MPa).

We cut circumferential notches in the borehole at the selected fracturing locations using a custom-designed mechanical system that will progressively extend carbide/polycrystalline-diamond cutters into the borehole wall. The notching systems include a device intended to be deployed on HQ-sized coring rod using the drill rig and rotated by the rig to cut the circumferential notch. The notch cutters extend diametrically using water pressure supplied by the drilling system. A schematic of the rig-deployed notch is provided in Figure 4.

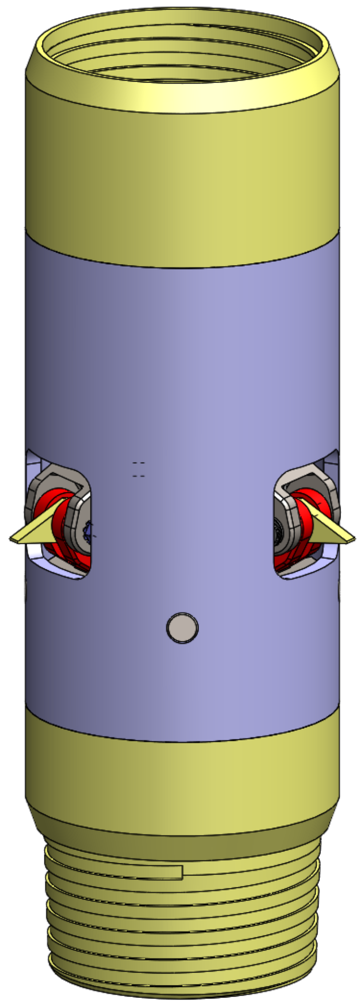

Figure 4: Rig-Deployed Notching Tool

4.3 Influence of Perturbed Stress Around Drift

The previous section discussed preliminary analysis assuming both homogeneous stress and elastic properties. In addition to stress variations associated with heterogenous rock properties, we expect systematic variations in thermal stress and mechanical stress due to the presence of the drift. Ventilation of the drift is expected to reduce the temperature in the surrounding rock, while the removal of material to engineer the drift itself creates stress relief. Figure 5 shows the temperature field (a) and the magnitude of minimum principal stress (b) along the expected fracture plane. The results show that the temperature perturbation caused by the drainage and ventilation history of the drift has reached the planned fracturing location and so has the corresponding stress alteration.

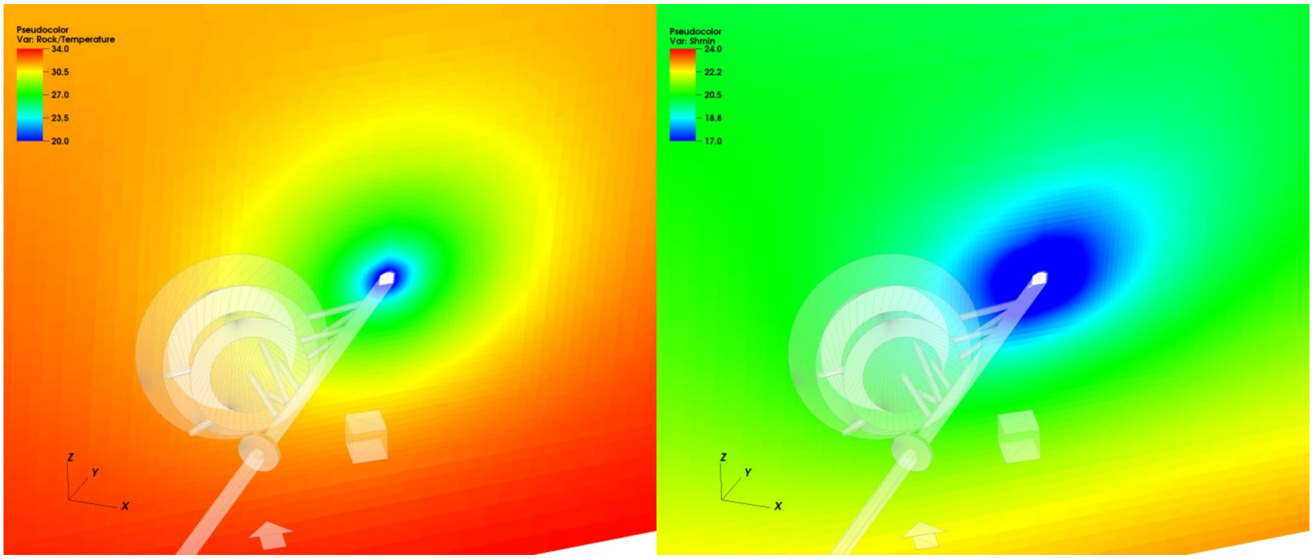

(a) (b)

Figure 5: The (a) temperature and (b) stress (minimum principal stress) perturbations caused by the drift along the expected fracture plane. The profiles of the drift, the planned wells, and the hypothetical fractures are shown in semi-transparency.

We modeled injection (where the hydraulic fracture is initiated) 38.4 m to the left of and 14.0 m below the axis of the drift. The distance between the injection point and the drift axis is approximately 51 m along the expected fracture plane. Water with a nominal viscosity of 1.0 cP is injected at a rate of 0.1 L/s, which is in the higher end of the planned stimulation rate. The critical stress intensity factor (K_{IC}, commonly known as the "toughness" of the rock) is assumed to be 1.0 MPa·$m^{0.5}$.

The simulated fracture shape and aperture distribution after 6 minutes (36 L total injected) of stimulation are shown in Figure 6. Shown in the background is the magnitude of the minimum principal stress in the rock body on a planar "slice" that is parallel to and 5 m away from the expected fracture plane. Instead of forming a "penny" shape around the stimulation well as the simplistic analysis indicates, the fracture shows a very strong tendency to grow toward the drift, driven by the strong gradient of S_{hmin}. The gradient is approximately 40 kPa/m at the fracture initiation point and increases as the fracture approaches the drift. The aperture near the injection point (0.15 mm) is close to the value estimated based on a toughness-dominated penny-shaped hydraulic fracture. The aperture is smaller at locations farther from the injection but could be larger when the fracture is near the drift, due to the very low local stresses. Note that this prediction did not include the production well, which would be expected to drain fluid from the fracture and reduce its propensity for propagation toward the drift.

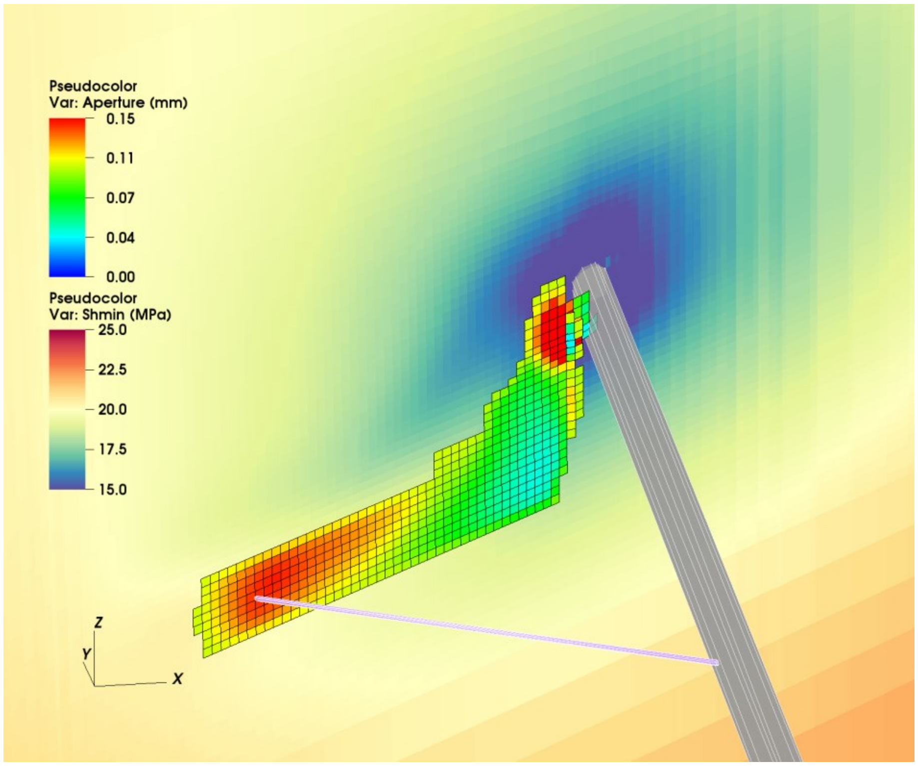

Figure 6 Fracture extents and aperture distribution after 6 minutes of injection at 0.1 L/s under the strong influence of the stress perturbation caused by the drift. Shown in the background is the magnitude of the minimum principal stress in the rock body on a planar "slice" that is parallel to and 5 m away from the expected fracture plane. The locations of the drift and the planned stimulation well are shown in the figure.

5. GEOPHYSICAL MONITORING DISCUSSION

Multiple methods will be employed to monitor the hydrofracture and flow-through experiments. We anticipate utilizing continuous active-source seismic monitoring (CASSM), passive microseismic (MEQ) monitoring, acoustic emissions (AE), electrical resistivity tomography (ERT), borehole pressure monitoring, in situ borehole deformation monitoring using the SIMFIP tool, and continuous distributed monitoring of temperature, seismicity, and strain using fiber optic cables. A number of these methods were successfully utilized in prior field experiments (e.g., Oldenburg et al., 2016; 2017; Knox et al., 2016). Each of these methods are described briefly below.

Continuous Active-Source Seismic Monitoring (CASSM): CASSM instrumentation will be deployed within the monitoring wells of Experiment 1. The instruments will operate both during the active fracturing, and in a background before and after fracturing events. The results are expected to be a measurement of stress sensitivity and a continuous monitoring of stress changes and fracture growth between the boreholes associated with the induced hydrofractures.

Passive Microseismic Monitoring: Microseismic (or micro-earthquake, MEQ) monitoring is a passive observation of small-scale seismic events. In EGS Experiment 1, MEQ monitoring will be conducted to measure induced seismicity from hydraulic fracturing activities (e.g., Pettitt et al., 2012). These include its triggers, magnitude and propagation in crystalline rocks. MEQ data can help to understand patterns of fracture developments, connectivity and the impacts from in-situ stress, rock fabric and existing fractures or discontinuities. MEQ monitoring at the EGS Collab site will be carried out using high sensitivity three component (3C) accelerometers that will be installed in the monitoring boreholes

Acoustic Emissions: Acoustic emissions (AE) monitoring is an approach very similar to MEQ monitoring described previously, targeting very high frequency seismic energy generated during tensile and shear failure of brittle materials. This method was employed very successfully for a similar set of experiments conducted at the Aspo experimental underground facility in Sweden (Zang et al. 2017). While similar in principle to MEQ, the higher frequencies of AE recording require (a) faster recording rates, often including triggering, (b) special purpose transducers tuned to the AE band, and (c) special attention to transducer installation to preserve higher frequency coupling. AE records, when processed, can provide information on periods of active fracturing through examination of event frequency. When integrated with an appropriate velocity model, AE events can be located to provide a time-resolved image of fracture advancement. Lastly, AE events can potentially be analyzed using moment tensor methods to evaluate failure modes.

Electrical Resistivity Tomography (ERT): In contrast to seismic data, ERT data are sensitive to changes in temperature, fluid saturation and fluid conductivity caused by fracture stimulation and flow. The objective of the ERT monitoring is to provide unique information for model validation by 1) imaging the conductivity distribution of the host rock prior to fracturing, as part of the initial characterization phase, 2) imaging the fracture extent by imaging the change in conductivity caused by the presence of fracture fluid and geophysical tracers within the fracture zone, 3) monitoring fracture fluid transport during fracture flow experiments using time-lapse imaging, and 4) monitoring the thermal zone of influence by imaging changes in bulk conductivity caused by temperature variation during a thermal flow test.

Borehole Deformation Monitoring: Deformation monitoring will be conducted in the injection well with the Step-rate Injection Method for Fracture In-situ Properties (SIMFIP - also called HPPP) tool. This tool is a unique 6-component optical strain system that allows a zone of a borehole to be hydraulically isolated by packers to allow standard fluid injection tests, while precisely monitoring deformations along and transverse to the borehole, and downhole injection pressures and flow rates from the fluid injection (Guglielmi et al., 2015).

Distributed temperature, seismicity, and strain monitoring: Distributed fiber optic sensing offers a cost-effective approach for monitoring a suite of physical properties continuously along monitoring wells. Distributed temperature (DTS), strain (DSS), and acoustic (DAS) sensing offer opportunities for geothermal monitoring due to their low deployment cost and excellent performance at high temperatures when appropriate packaging is chosen. We are deploying several multi - fiber cables to measure these properties, focusing on grouted cables in the monitoring boreholes. The DSS datasets, particularly data acquired in the fracture orthogonal wells, will provide constraints on fracture intersection in any of the 6 monitoring boreholes. The DTS recording will provide additional constraints on the evolving temperature field during the thermal tests.

6. FLOW TESTING

One of the key objectives of Experiment 1 is to develop predictive models for fluid flow that can be tested by well-constrained field experiments. We plan to conduct several flow and tracer tests that will provide critical information regarding the generation of permeable fractures for EGS reservoirs. Each flow test will be conducted within the fracture zone between the stimulation well and a production well. Both the stimulation and production wells will be instrumented with a packer system and sensors that monitor fracture aperture and shear, as well as temperature and pressure above, below, and within the isolated interval. These tests will be preceded by numerical modeling simulations to help design the flow, thermal and tracer testing (Figure 7).

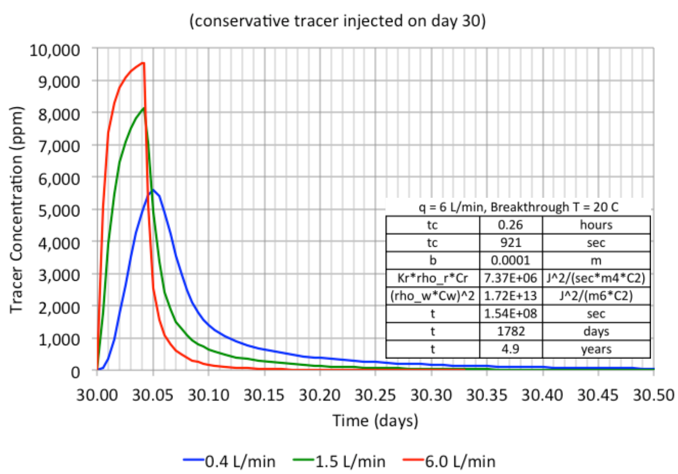

Figure 7: Simulations of conservative tracer test results for a variety of injection rates.

The objective of the first flow test is to determine the fracture propagation pressure, which will provide the pressure boundary constraints necessary to reduce the risk of continued fracture propagation during flow testing. The second test is an isothermal step pressure test, whereby the response of the fracture aperture and flow as a function of pressure will be determined. The third test will be a constant rate flow test with both conservative and reactive tracers. The objective of this test is to interrogate fracture residence time and surface area. The analysis of chemical tracers will be one technique used to determine injected fluid residence time and the apparent fracture surface area. Conservative tracers (e.g. NaCl, KCl, NaI, sodium fluorescein, naphthalene sulfonates, and DNA fragments) will be used to determine residence times. Reactive tracers (e.g. rhodamine B, FD&C dyes) that temporarily absorb to the rock will be used to assess the fracture rock surface area. Depending on results of the first test, two or more constant rate tests may be conducted to investigate residence time as a function of fracture aperture. The objective of the fourth test is to investigate thermal transfer and stress effects during cold water injection. This test is expected to last several weeks, and will require full automation of injection and monitoring systems.

7. CONCLUSIONS AND IMPLICATIONS FOR EXPERIMENT DESIGN

We have provided an overview of our objectives and approach to designing the first experimental testbed of the EGS Collab project. This first experiment has the goal of providing excellent observations of stimulation and subsequent flow-through tests. Although our initial preferred site geometry involved intersecting drifts (to provide access for stimulation and orthogonal monitoring boreholes), we identified a new testbed design that allows us to achieve a similar borehole layout from a single drift running at an angle to the principal stress directions. Preliminary analytic solutions indicate that approximately 60 L of water injected would be expected to induce a tight fracture (approximately 150 microns in aperture) of 15 m radius, consistent with previous injections of similar magnitude in similar formations. More elaborate modeling, including thermomechanical effects due to cooling of the drift combined with stress relief at the free surface indicate that the hydraulic fracture may in fact develop a strong anisotropic propagation toward the drift. This may limit the volume of fluid that can be injected during the stimulation phase if we are to avoid the hydraulic fracture intersecting the drift (although the presence of the producing borehole may limit such propagation). However, this relationship between thermomechanics and fracture propagation presents a unique validation opportunity. If proven correct, rather than the fracture propagation being dictated by difficult-to-characterize local stress variations associated with elastic heterogeneity, the fracture propagation may be driven by a well-characterized stress gradient. Regardless of the induced fracture geometry, the combination of geophysical systems (CASSM, MEQ, AE, ERT, SIMFIP, DAS, DTS) and flow tests (thermal and various tracers) are intended to provide an excellent dataset for the community to use for the purpose of model validation. Finally, while this paper provides an overview of the experiment design and design process, separate papers will provide more details regarding the characterization of the site, the monitoring system, and other aspects of the project.

ACKNOWLEDGMENTS:

This manuscript has been authored by Lawrence Livermore National Security, LLC under Contract No. DE-AC52-07NA2 734-I with the US. Department of Energy. This research was supported by the U.S. Department of Energy, Office of Energy Efficiency and Renewable Energy (EERE), Office of Technology Development, Geothermal Technologies Office. The United States Government retains, and the publisher, by accepting the article for publication, acknowledges that the United States Government retains a non-exclusive, paid-up, irrevocable, world-wide license to publish or reproduce the published form of this manuscript, or allow others to do so, for United States Government purposes. The research supporting this work took place in whole or in part at the Sanford Underground Research Facility in Lead, South Dakota. The assistance of the Sanford Underground Research Facility and its personnel in providing physical access and general logistical and technical support is acknowledged.

REFERENCES

Allis, R., Moore, J., Davatzes, N., Gwynn, M., Hardwick, C., Kirby, S., McLennan, J., Pankow, K., Potter, S., and Simmons, S. (2016) EGS concept testing and development at the Milford, Utah FORGE site. Proceedings, 41st Workshop on Geothermal Reservoir Engineering, Stanford University, SGP-TR-209, 13 p.

Blankenship, D., Kennedy, M., Majer, E.L., Hinz, N., Faulds, J., Ayling, B., Blake, K., Tiedeman, A., Sabin, A., Lazaro, M., Akerley, J., Siler, D., Kaven, J.O, Phelps, G., Hickman, S., Glen, J., Williams, C., Robertson-Tait, A., Hackett, L., Pettitt, W. (2017) Proposed Fallon FORGE site: Phase 2 update. Proceedings, 42nd Workshop on Geothermal Reservoir Engineering, Stanford University, SGP-TR-212, 7 p.

Bunger, A.P.: *Near-Surface Hydraulic Fracture*, (2005), doctoral dissertation, University of Minnesota, Minneapolis, MN.

Detournay, E. (2004). Propagation Regimes of Fluid-Driven Fractures in Impermeable Rocks. International Journal of Geomechanics, 4(1), 35.

Guglielmi Y., Cappa F., Avouac J.P., Henry P., and Elsworth D. (2015). Seismicity triggered by fluid‐injection induced aseismic slip. Science 348, 1224; DOI: 10.1126/science.aab0476.

Guo, B., Fu, P., Y. Hao, Peters, C.A., and Carrigan, C.R.: Thermal drawdown-induced flow channeling in a single fracture in EGS, *Geothermics*, 61, (2016), 46–62.

Hart, K., Trancynger, T.C., Roggenthen, W., & Heise, J. (2014) Distribution modeling in support of physics experiments at the Sanford Underground Research Facility (SURF). Proceedings of the South Dakota Academy of Science, 93, 33-41.

Heise, J. (2015). The Sanford Underground Research Facility at Homestake, Journal of Physics: Conference Series. Vol. 606. No. 1, IOP Publishing.

Huang, L., Chen, Y, Gao, Fu, P., Morris, J, Ajo-Franklin, J, Nakagawa, S, and EGS Collab Team, Numerical Modeling of Seismic and Displacement-Based Monitoring for the EGS Collab Project, Geothermal Resources Council Transactions, v. 41, (2017).

Hubbert, K. M., and Willis, D. G.: Mechanics of Hydraulic Fracturing, Transactions of the American Institute of Mining, Metallurgical, and Petroleum Engineers, (1957), 210(6), 153–163.

Juvonen, L., 2002, Rock mechanics studies at underground research laboratories for spent nuclear fuel repositories - literature survey, Working Report 2002-55, http://www.posiva.fi/files/2174/POSIVA-2002-55_Working-report_web.pdf

Knox, H.A., Ajo-Franklin, J.B., Johnson, T.C., Morris, J.P., Grubelich, M.C., Preston, L.A., Knox, J.M., and King, D. (2016) High energy stimulations imaged with geophysical change detection techniques. Geothermal Resources Council Transactions, 40, 361-371.

Nolte, K. G. (2000). Reservoir stimulation (Vol. 18). M. J. Economides (Ed.). New York: Wiley.

Oldenburg, C.M., Dobson, P.F., Wu, Y., Cook, P.J., Kneafsey, T.J., Nakagawa, S., Ulrich, C., Siler, D.L., Guglielmi, Y., Ajo-Franklin, J., Rutqvist, J., Daley, T.M., Birkholzer, J.T., Wang, H.F., Lord, N.E., Haimson, B.C., Sone, H., Vigilante, P., Roggenthen, W.M., Doe, T.W., Lee, M.Y., Ingraham, M., Huang, H., Mattson, E.D., Zhou, J., Johnson, T.J., Zoback, M.D., Morris, J.P., White, J.A., Johnson, P.A., Coblentz, D.D., and Heise, J. (2016) Intermediate-Scale Hydraulic Fracturing in a Deep Mine – kISMET Project Summary 2016. LBNL Report 1006444, 114 p.

Oldenburg, C.M., Dobson, P.F., Wu, Y., Cook, P.J., Kneafsey, T.J., Nakagawa, S., Ulrich, C., Siler, D.L., Guglielmi, Y., Ajo-Franklin, J., Rutqvist, J., Daley, T.M., Birkholzer, J.T., Wang, H.F., Lord, N.E., Haimson, B.C., Sone, H., Vigilante, P., Roggenthen, W.M., Doe, T.W., Lee, M.Y., Ingraham, M., Huang, H., Mattson, E.D., Zhou, J., Johnson, T.J., Zoback, M.D., Morris, J.P., White, J.A., Johnson, P.A., Coblentz, D.D., and Heise, J. (2017) Hydraulic fracturing experiments at 1500 m depth in a deep mine: Highlights from the kISMET project. Proceedings, 42nd Workshop on Geothermal Reservoir Engineering, Stanford University, Feb. 13-15, 2016, 9 p.

Pettitt, W.S., Pierce, M., Damjanac, B., Hazzard, J., Lorig, L., Fairhurst, C., Sanchez-Nagel, M., Nagel, N., Reyes-Montes, J.M., Andrews, J., and Young, R.P. (2012) Fracture network engineering: Combining microseismic imaging and hydrofracture simulations. 46th US Rock Mechanics / Geomechanics Symposium, ARMA 12-554, 9 p.

Settgast, R.R., Fu, P., Walsh, S.D.C., White, J.A., Annavarapu, C., and Ryerson F. J.: A fully coupled method for massively parallel simulation of hydraulically driven fractures in 3-dimensions, Int. J. Numer. Anal. Methods Geomech., (2017), 41(5), 627–653.

Sneddon, I. N. (1946). The Distribution of Stress in the Neighbourhood of a Crack in an Elastic Solid. Proceedings of the Royal Society A: Mathematical, Physical and Engineering Sciences, 187(1009), 229–260.

Sneddon, I., and Elliott, H. (1946). The opening of a griffith crack under internal pressure. Quarterly of Applied Mathematics, 4(3), 262–267.

Wang, H.F., Lee, M.Y., Doe, T.W., Haimson, B.C., Oldenburg, C.M., and Dobson, P.F. (2017) In-situ stress measurement at 1550-meters depth at the kISMET test site in Lead, S.D. Proceedings, 51st US Rock Mechanics / Geomechanics Symposium, American Rock Mechanics Association, ARMA 17-000651, 7 p.

White, M, Fu, P, Huang, H, Ghassemi, A, and EGS COLLAB Team, The Role of Numerical Simulation in the Design of Stimulation and Circulation Experiments for the EGS Collab Project, Geothermal Resources Council Transactions, v. 41, (2017).

Zang, A., Stephansson, O., Stenberg, L., Plenkers, K., Specht, S., Milkereit, C., Schill, E., Kwiatek, G., Dresen, G., Zimmermann, G. and Dahm, T., 2017. Hydraulic fracture monitoring in hard rock at 410 m depth with an advanced fluid-injection protocol and extensive sensor array. Geophysical Journal International, 208(2), pp.790-813.

Zhou, J., Huang, H., Mattson, E., Doe, T.W., Oldenburg, C.M., Dobson, P.F., and Wang, H.F. (2017) Post-fracturing experiment simulation of hydraulic fracture propagation in a deep mine using a fully coupled 3D network-flow and quasi-static discrete element model. Proceedings, 51st US Rock Mechanics / Geomechanics Symposium, American Rock Mechanics Association, ARMA 17-000651, 9 p.

Ziagos, J., Phillips, B.R., Boyd, L., Jelacic, A., Stillman, G., and Hass, E. (2013) A technology roadmap for strategic development of Enhanced Geothermal Systems. Proceedings, 38th Workshop on Geothermal Reservoir Engineering, Stanford University, SGP-TR-198, 24 p.